Morphosynthesis of Nacre-Type Laminated $CaCO_3$ Thin Films and Coatings**

Dirk Volkmer, Marc Harms, Laurie Gower, and Andreas Ziegler*

$CaCO_3$ is one of the most abundant biogenic minerals. Biological organisms utilize mainly the thermodynamically most stable crystal polymorphs of $CaCO_3$, that is, calcite or aragonite, for the construction of protective shells and casings.[1] Among the many intricate shapes and architectures of naturally occurring biominerals, the structure and properties of nacre ("mother-of-pearl"), the iridescent inner layer of mollusc shells, has had a special attraction for scientists. Nacre consists of stacked layers of tabular aragonite crystals that are interspersed with a thin organic matrix. Investigations on the ultrastructure of nacre suggest that mineral bridges exist between adjacent layers of aragonite crystals and, therefore, the highly uniform coorientation of the crystals is maintained over long distances.[2] The unique crystal texture of nacre gives rise to unusual material properties such as toughness, corrosion resistance, and its characteristic luster.[3] Noteworthy, this laminated crystal texture sometimes is found in (fossil) brachiopods, which, however, are made up of thin layers of calcite instead of aragonite crystals.[4,5]

Many investigations have focussed on the biosynthesis of nacre to elucidate the mechanisms by which the mollusc gains control over the selection of the $CaCO_3$ polymorph, the shape and the size of individual crystals, and their integration into a brickwork-like pattern. It has been proposed that the organic matrix acts as a template for the nucleation of a first layer of aragonite crystals.[6] Reconstitution experiments[7] employing macromolecules extracted from different sites of de-mineralized mollusc shells indicate that the selection of $CaCO_3$ polymorph might be triggered by specific soluble peptides that have an unusually high content of acidic amino acid side chains.[8] Moreover, model systems employing self-assembled monolayers (SAMs) of carboxy-terminated alkylthiols bound to Au or Ag surfaces have impressively demonstrated that the growth orientation of calcite crystals might be well controlled by virtue of a geometrical or stereochemical match between the carboxylate moieties of the immobilized SAM and the juxtaposed calcite crystal face.[9] However, this approach as yet has not proven to be applicable for the construction of nacre-type materials, in which both the laminated structure can be achieved, as well as control over crystal orientation and phase. Complementary investigations by our group,[10] among others,[11] in which non-immobilized monolayers of amphiphilic macrocycles were employed, on the other hand have shown that the average charge distribution at the template surface is the predominant factor that governs the selection of crystal polymorphs and the orientation of crystals.

We present here an alternative process for synthesizing a highly organized nacre-type material (Figure 1). This novel morphosynthetic approach[12] rests on the deposition of a polycrystalline calcite thin film starting from a metastable amorphous precursor phase. The polycrystalline thin film, in turn, serves as a template upon which highly oriented layers of calcite crystals are deposited under nonequilibrium conditions.

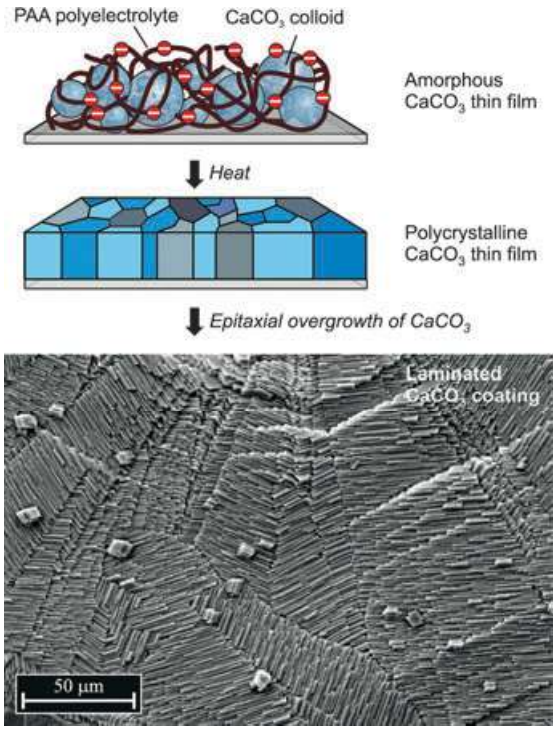

Figure 1. Scheme of a three-step procedure for the morphosynthesis of nacre-type laminated $CaCO_3$ coatings. In the first step an amorphous highly hydrated $CaCO_3$ thin film is deposited on a glass substrate. Upon heating this precursor film is transformed into a polycrystalline thin film consisting of a mosaic of flat single-crystalline calcite domains. In the last step highly oriented single and multiple layers of calcite crystals are grown epitaxially on the underlying polycrystalline thin film.

[*] Prof. Dr. D. Volkmer, M. Harms
Inorganic Chemistry II
University of Ulm
Albert-Einstein-Allee 11, 89081 Ulm (Germany)
Fax: (+49) 731-50-23039
E-mail: dirk.volkmer@chemie.uni-ulm.de
Prof. Dr. L. Gower
Department of Materials Science & Engineering
University of Florida
P.O. Box 116400, Gainesville (USA)
Priv.-Doz. Dr. A. Ziegler
Central Faculty of Electron Microscopy
University of Ulm
Albert-Einstein-Allee 11, 89069 Ulm (Germany)

[**] This work was financially supported by the Deutsche Forschungsgemeinschaft (DFG Schwerpunktprogramm 1117, "Prinzipien der Biomineralisation"; DFG grant Vo829/2-1). The authors are grateful to R. Oldenbourg (Marine Biological Laboratory, Woods Hole, USA) for helpful comments on LC-PolScope data analysis.

In a typical experiment, a supersaturated solution of $CaCO_3$ continuously flows through a perfusion cell mounted on a microscope stage. A constant supersaturation level is maintained by feeding a 10 mM solution of $CaCl_2$ and Na_2CO_3 into a mixing chamber that is connected to the inlet port of a perfusion cell. (A complete description of the experimental set-up is given in the Supporting Information). In the first step an amorphous $CaCO_3$ precursor film is deposited on the surface of the glass slides that are at the top and the base of the perfusion cell. An anionic polymer is added to the Na_2CO_3 solution that serves as a process-directing agent which induces liquid–liquid phase separation and ultimately deposition of an amorphous precursor film.[13] Preliminary investigations on the influence of the polyelectrolytes's molecular weight, its concentration, and its chemical nature showed us that low-molecular-weight atactic poly(acrylic acid) (PAA, av $M_w = 2100\ g\,mol^{-1}$; 8.0×10^{-3} wt%) is most suitable for stabilizing amorphous $CaCO_3$ precursor films on glass substrates. The amorphous thin film displays characteristic alterations of its optical density ("meander texture", Figure 2a). Scanning electron micrographs (Figure 2b–d) taken from different film regions indicate that the meander texture is due to an irregular distribution of granular matter, which is presumably caused by a turbulent flow of solution in the perfusion cell. At higher magnifications it is clearly seen that the amorphous thin film consists of aggregated colloid particles with a narrow size dispersion between 20–30 nm. The IR spectrum of the amorphous thin film shows a broad split peak at 1479 and 1419 cm^{-1} and a weak band appearing at around 675 cm^{-1}, which demonstrates that the colloid particles mainly consist of amorphous $CaCO_3$.[14]

If the mother liquor is removed and the coated substrate is subjected to drying at room temperature for several days, the amorphous $CaCO_3$ thin film partially transforms into the crystalline state. However, a complete transition is readily achieved if the amorphous precursor thin film is heated at 400 °C for about 2 h. This yields an optically birefringent thin film of constant thickness (typically 500–700 nm), the polarization optical micrograph of which reveals a characteristic mosaic structure (Figure 3a). Domains appearing homogeneous in the polarization optical micrograph are separated by cracks that develop during the drying/heating procedure. Scanning electron micrographs (Figure 3b,c) reveal that the amorphous $CaCO_3$ colloid particles have coalesced to form an almost homogeneous crystalline thin film. These results are complemented by atomic force microscopy (AFM) surface topography images (see Supporting Information), which demonstrate that the film surface is not atomically flat, but retains a rough surface (rms surface roughness $R_q = 16.90\ nm^{-1}$) that is commensurate to the size of the $CaCO_3$ colloid particles found in the precursor film.

The mineral phase was characterized by IR spectroscopy and X-ray diffraction. The three bands observed in the IR spectrum at $\tilde{\nu} = 1415$, 875, and 711 cm^{-1} are characteristic of crystalline calcite.[14] X-ray diffraction yields sharp peaks that can be assigned to the XRD pattern of calcite (see Supporting Information).[15] There is no indication of other $CaCO_3$ polymorphs (aragonite, vaterite) being formed upon heating the sample. The relative intensities of the observed XRD peaks, however, differ only slightly from those of a calcite powder reference sample, the most notable deviation being

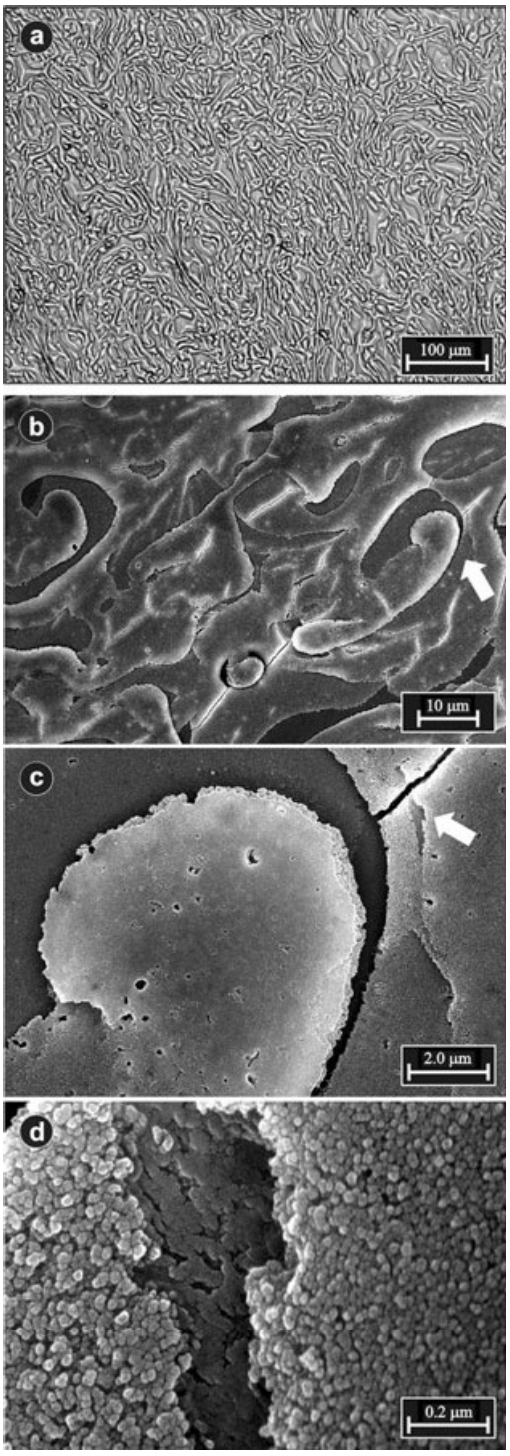

Figure 2. a) Optical texture of an amorphous $CaCO_3$ precursor thin film grown after 45 min on a glass cover slide under constant perfusion (0.75 mL min^{-1}) of a supersaturated solution of $CaCO_3$ (10 mM $CaCl_2$, 10 mM Na_2CO_3, 8.0×10^{-3} wt% PAA ($M_w = 2100\ g\,mol^{-1}$, $T = 295$ K). (Bright field optical micrograph, digital contrast enhancement). b–d) Scanning electron micrographs of the film at different magnifications showing a meander texture of aggregated amorphous $CaCO_3$ colloid particles. (White arrows point to the approximate image area shown at the next higher magnification level).

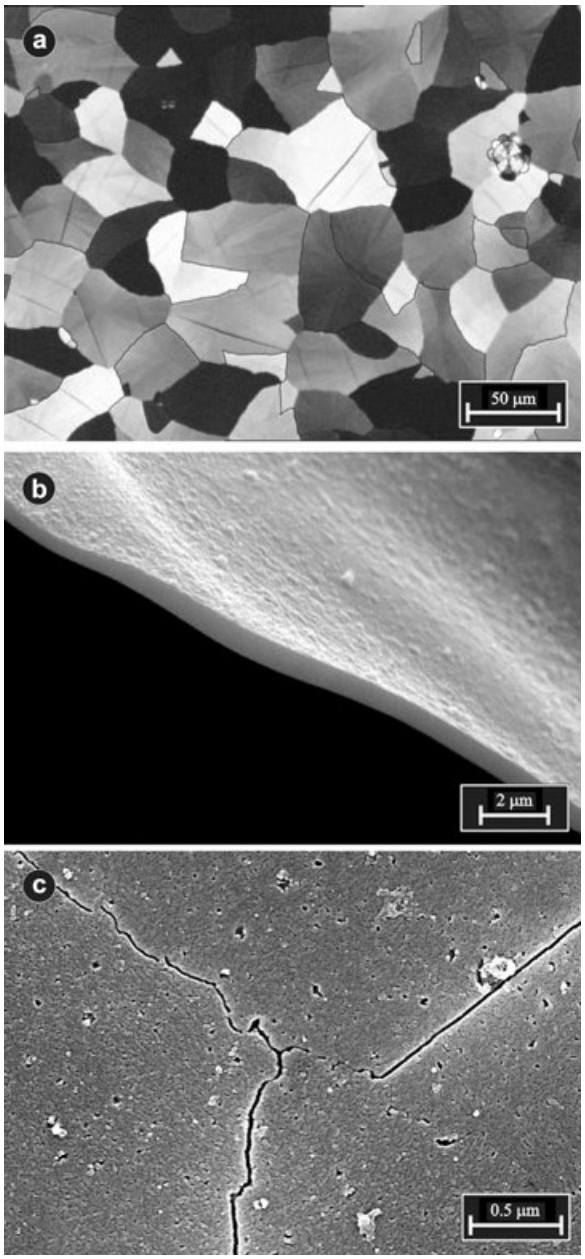

Figure 3. a) Polarization optical micrograph of a polycrystalline $CaCO_3$ thin film obtained from an amorphous precursor film after heating at 400°C for 2 h. The observed mosaic structure of the thin film is due to the presence of discrete domains each consisting of a flat calcite single crystal. The typical domain sizes range from 50–200 μm in diameter. b,c) Scanning electron micrographs of a polycrystalline $CaCO_3$ thin film obtained from an amorphous precursor film after heating at 400°C for 2 h. The film thickness was measured at the edge of films where pieces occasionally lifted off the substrate surface. The average film thickness is 600 nm (±100 nm).

the slightly weakened intensity of the calcite (10.4) peak. However, the XRD pattern of the polycrystalline calcite thin film does not show any exceptional preference in favor of a single crystal orientation.

Digital image analysis of the polarization optical micrographs taken from a polycrystalline calcite thin film mounted between crossed polarizers shows that for each individual domain an almost constant gray level can be assigned. This behavior can be easily understood if we assume that each domain constitutes a calcite single crystal that arises from a singular nucleation event occurring within the amorphous precursor film, the orientation of which differs from that of its neighbor(s). To demonstrate the single-crystalline nature of the domains, $CaCO_3$ overgrowth experiments were performed, by using the polycrystalline thin film as an isoepitaxial substrate.[16] Thus, a glass slide carrying the polycrystalline thin film was subjected once again to a continuous flow of supersaturated $CaCO_3$ solution, which at this time was lacking the PAA inhibitor. To our delight, single and multiple layers of highly oriented calcite crystals grew on top of the polycrystalline thin film, thus leading to a notable iridescence. Marked areas of the polycrystalline thin films were examined by polarization optical microscopy as well as by scanning electron microscopy before and after calcite overgrowth had taken place (Figure 4). The micrographs clearly show that the underlying flat calcite domains direct the orientation of the overgrowing polycrystalline calcite layer. The crystal texture changes abruptly at the borderline between different domains but stays constant within each individual domain area. Within many domains calcite crystals are grown together forming stacks of perfectly co-aligned platelets. Determining the crystal growth orientation in different domains is straightforward since the rhombohedral calcite morphology is preserved in all cases.[17] Figure 4c,d shows the representative details of oriented calcite layers thus obtained. When the growth of the calcite layer onto the polycrystalline film is interrupted after 45 min, the crystals have a narrow thickness distribution typically ranging from 700 to 1200 nm. (The maximum film thickness thus achievable is about 4.5–5.8 μm after 12 h.). We currently anticipate that the combination of mesoscopic size and parallel periodic arrangement of the crystals leads to the glistening appearance of the samples.

To gain deeper insights into the structure-directing role of the polycrystalline $CaCO_3$ thin film obtained from the amorphous precursor film, we employed a novel optical birefringence imaging system (LC-PolScope).[18] This system provides a means to visualize and measure retardance magnitude and slow-axis orientation at every pixel of a charge-coupled device (CCD) image within seconds. Since calcite is a uniaxial birefringent material, a thin calcite platelet will lead to an optical retardance value that depends on the sample thickness and the orientation of the crystallographic c axis (= optical axis) with respect to the direction of the polarized light beam propagating through the sample. The retardance δ (in nm) of a uniformly thin calcite platelet is given by Equation (1)[19], where ϑ is the angle between the

$$\delta = \rho(n_e - n_o)\sin^2\theta \qquad (1)$$

optical axis and the propagation direction of the beam, ρ (in nm) is the thickness of the crystal sheet and $(n_e - n_o)$ the birefringence of calcite (ca. -0.174 at $\lambda = 546.5$ nm).[20] Thus, measuring the optical retardance of many different calcite domains simultaneously yields information about the frequency by which different crystal orientations occur in the polycrystalline thin film obtained from the amorphous

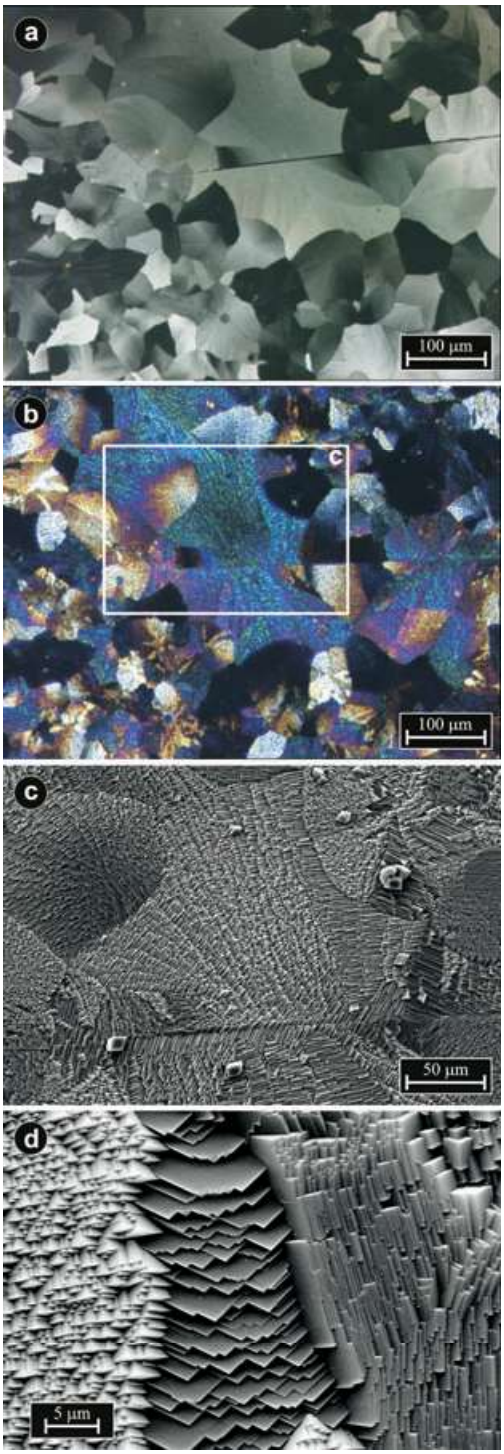

Figure 4. Highly oriented laminated calcite layers grown on a flat calcite thin film. Optical micrographs of a polycrystalline calcite thin film mounted between crossed polarizers before (a) and after calcite overgrowth (b). Scanning electron micrographs showing details of the crystal texture (c, d). d) Detail of a calcite layer showing abrupt changes of crystal orientations at the domain boundaries. Growth directions were tentatively assigned by measuring the projected interfacial angles of the calcite rhombohedra in the micrograph and comparing these to calculated values. (Left: $<00.1>$, middle: $<01.8>$, right $<11.0>$)

precursor. Unfortunately, for materials possessing uniaxial birefringence, the ϑ value cannot be assigned to a unique crystallographic direction. However, it is possible to calculate retardance values for characteristic calcite crystal orientations that are frequently observed in calcite overgrowth experiments. Figure 5a shows an LC-PolScope pseudo-color repre-

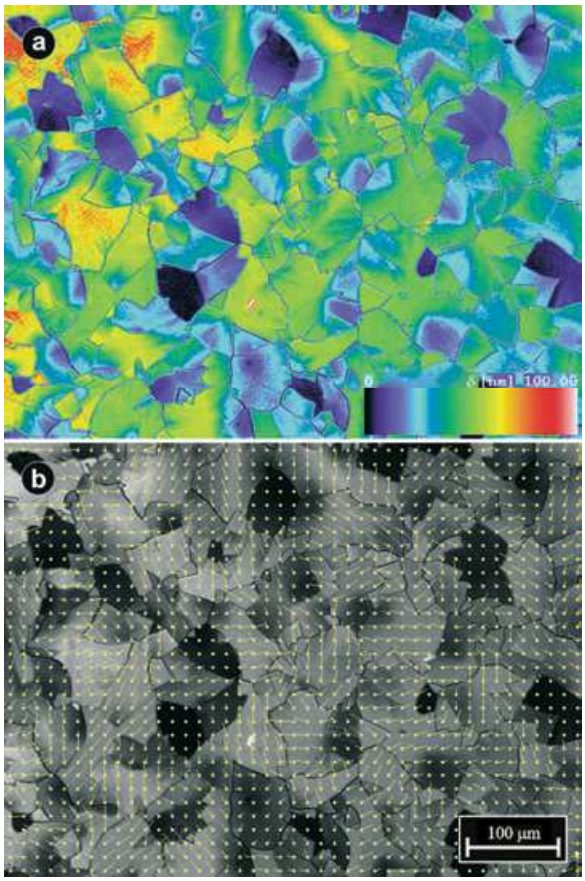

Figure 5. a) LC-PolScope image of a polycrystalline calcite thin film (retardance given as pseudo-color). b) Retardance grayscale image overlaid by short lines indicating the orientations of the slow birefringence axis measured in each location. (Slow axis orientations are typically shown for every 15 pixel in the horizontal and vertical direction of the original video frame).

sentation of optical retardance values δ of a polycrystalline thin film measured for each point of the image. Note that experimental δ values differ from domain to domain, but stay nearly constant within each individual domain. (Some calcite domains show a biaxial birefringence pattern that might be stress-induced, presumably caused by the shrinkage occurring during the drying process which is necessary to transform the highly hydrated amorphous precursor into an anhydrous polycrystalline thin film.) The most frequent retardance values cluster around $80(\pm 5)$, $49(\pm 4)$, $20(\pm 3)$, $15(\pm 2)$, and $0(\pm 2)$ nm. The best matching calculated retardance values are 82.1 {01.2}, 50.9 {01.4}, 20.2 {10.10}, 13.6 {01.8}, and 0 nm {00.1} for a sample thickness of 600 nm, (the crystal face which is parallel to the glass substrate, or perpendicular to the light direction, respectively, is given in braces).[21] Figure 5b displays the same film area with the direction of the slow birefringence axis indicated as small vectors at different points. Note that most domains within the mosaic thin film are

uniformly oriented.

LC-PolScope imaging of polycrystalline calcite thin films yields two important features: First, there is strong evidence that the polycrystalline calcite thin films in fact consist of flat single crystals. The crystal orientation switches at the domain boundaries, but there is no preference for a particular orientation, which is in agreement with the results of XRD measurements. Second, experimental retardance values are fully consistent with theoretical ones, based on crystal orientations that we have observed in crystal overgrowth experiments (Figure 4d). These findings lead us to conclude that calcite overgrowth most likely occurs by isoepitaxy, which is, however, somewhat unexpected, considering the mesoscopic surface roughness of the underlying polycrystalline thin film (Figure 3c).

The preparation of biologically inspired laminates mimicking the architectural concept of nacre, albeit at a somewhat smaller length scale, has been described previously.[22] Amorphous $CaCO_3$ thin films have been grown underneath Langmuir monolayers in the presence of PAA,[23] and their formation has been monitored in situ by synchrotron reflectivity studies.[23b] The effects of functional groups of insoluble biopolymers on $CaCO_3$ thin film formation have been investigated,[24] and the formation of aragonite thin films on chitosan matrices in the presence of Mg^{2+} ions and poly-Asp (Asp = aspartic acid) has been demonstrated.[25] However, as yet none of these approaches has led to highly oriented laminated crystal architectures similar to those reported here. Our investigations show that nacre-type $CaCO_3$ thin films and coatings can be obtained by a morphosynthetic approach[26] that requires *no* structurally preorganized organic matrix. The key steps involve the transformation of an amorphous $CaCO_3$ precursor thin film into a polycrystalline calcite thin film, which, in turn, serves as a template for epitaxial overgrowth of highly oriented layers of uniform calcite platelets. This strategy leads to a general, technically feasible approach towards highly ordered materials consisting of microcrystals with typical sizes ranging from a few tens to a few hundreds of nm, which could be technologically interesting for photonic applications, for example for diffraction gratings,[27] photonic band gap materials,[28] and coatings based on structural colours instead of pigments.[29]

In terms of rationalizing the formation of highly organized crystal textures in biological organisms, our investigations might provide an alternative concept as opposed to the commonly believed structure-directing role of organic templates in biomineralization. It is thus imaginable that highly organized crystal architectures such as nacre or the foliated and prismatic layers, may grow spontaneously and continuously once a first crystal layer has been deposited, requiring no further elaborate control mechanisms.[30] However, the transition of an amorphous precursor into crystalline polymorphs is a key step involved in many biomineralization processes, and the mechanism(s) by which organisms trigger this particular transformation are largely unknown.[31]

The availability of a nondestructive, real-time retardance imaging system such as the LC-PolScope used here represents a significant addition to analytical tools available for characterizing the amorphous–solid state transition of (inorganic) materials in situ. Investigations are underway to find the appropriate experimental conditions under which regular biomimetic $CaCO_3$ architectures constructed from aragonite instead of calcite can be produced.

[1] H. A. Lowenstam, S. Weiner, *On Biomineralization*, Oxford University Press, New York, **1989**.

[2] a) S. W. Wise, *Science* **1970**, *167*, 1486–1488; b) H. K. Erben, N. Watabe, *Nature* **1974**, *248*, 128–130; c) T. E. Schaffer, C. Ionescu-Zanetti, R. Proksch, M. Fritz, D. A. Walters, N. Almqvist, C. M. Zaremba, A. M. Belcher, B. L. Smith, G. D. Stucky, D. E. Morse, P. K. Hansma, *Chem. Mater.* **1997**, *9*, 1731–1740; d) X. Su, A. M. Belcher, C. M. Zaremba, D. E. Morse, G. D. Stucky, A. H. Heuer, *Chem. Mater.* **2002**, *14*, 3106–3117.

[3] a) J. D. Currey, *Proc. R. Soc. London* B **1977**, *196*, 443–463; b) A. P. Jackson, J. F. V. Vincent, R. M. Turner, *Proc. R. Soc. London* B **1988**, *234*, 415–440; c) A. G. Evans, Z. Suo, R. Z. Wang, I. A. Aksay, M. Y. He, J. W. Hutchinson, *J. Mater. Res.* **2001**, *16*, 2475–2484.

[4] K. M. Towe, C. W. Harper, *Science* **1966**, *154*, 153–155.

[5] A comparable architecture is found in non-molluscan species such as bryozoan lophophorates, in which laminated calcite tablets are referred to as seminacre since they are less organized than the nacre of molluscs. M. J. Weedon, P. D. Taylor, *Biol. Bull.* **1995**, *188*, 281–292.

[6] a) S. Weiner, W. Traub, *Phil. Trans. R. Soc. Lond.* B **1984**, *304*, 425–433; b) S. Mann, *Nature* **1988**, *332*, 119–124; c) Y. Levi-Kalisman, G. Falini, L. Addadi, S. Weiner, *J. Struct. Biol.* **2001**, *135*, 8–17.

[7] a) G. Falini, S. Albeck, S. Weiner, L. Addadi, *Science* **1996**, *271*, 67–69; b) Y. Levi, S. Albeck, A. Brack, S. Weiner, L. Addadi, *Chem. Eur. J.* **1998**, *4*,389–396.

[8] a) P. E. Hare, *Science* **1963**, *139*, 216–217; b) B. A. Gotliv, L. Addadi, S. Weiner, *ChemBioChem* **2003**, *4*, 522–529.

[9] a) J. Aizenberg, J. A. Black, G. M. Whitesides, *J. Am. Chem. Soc.* **1999**, *121*, 4500–4509; b) A. M. Travaille, L. Kaptijn, P. Verwer, B. Hulsken, J. A. A. W. Elemans, R. J. M. Nolte, H. van Kempen, *J. Am. Chem. Soc.* **2003**, *125*, 11571–11577.

[10] a) D. Volkmer, M. Fricke, D. Vollhardt, S. Siegel, *J. Chem. Soc. Dalton Trans.* **2002**, 4547–4554; b) D. Volkmer, M. Fricke, C. Agena, J. Mattay, *J. Mater. Chem.* **2004**, *14*, 2249–2259.

[11] a) M. J. Lochhead, S. R. Letellier, V. Vogel, *J. Phys. Chem. B* **1997**, *101*, 10821–10827; b) P. Calvert, S. Mann, *Nature* **1997**, *386*, 127–129.

[12] D. Volkmer, S. Tugulu, M. Fricke, T. Nielsen, *Angew. Chem.* **2003**, *115*, 60–64; *Angew. Chem. Int. Ed.* **2003**, *42*, 58–61.

[13] L. B. Gower, D. J. Odom, *J. Cryst. Growth* **2000**, *210*, 719–734.

[14] The strong band at $\tilde{\nu}_3 = 1415\ cm^{-1}$ can be assigned to the asymmetric C–O stretching mode of CO_3^{2-} in calcite while those centred at $\tilde{\nu}_2 = 875\ cm^{-1}$ corresponds to the CO_3^{2-} out-of-plane deformation mode. The band at $\tilde{\nu}_4 = 711\ cm^{-1}$ corresponds to the O-C-O bending mode of crystalline calcite. F. A. Andersen, L. Brecevic, *Acta Chem. Scand.* **1991**, 1018–1024.

[15] Crystallographic indices are presented in three-index (*hk.l*) notation, based on the hexagonal setting of the calcite unit cell ($R\bar{3}c$, $a = 4.96$, $c = 17.002$ Å).

[16] This technique has been used by others to determine the crystal orientation of underlying biogenic crystals that lack facets due to their nonequilibrium morphologies: a) K. Okazaki, R. M. Dilla-

man, K. M. Wilbur, *Biol. Bull.* **1981**, *161*, 402–415; b) J. Aizenberg, S. Albeck, S. Weiner, L. Addadi, *J. Cryst. Growth* **1994**, *142*, 156–164.

[17] D. D. Archibald, S. B. Qadri, B. P. Gaber, *Langmuir* **1996**, *12*, 538–546. A projection of rhombohedral faces onto the image plane of the micrograph yields characteristic interfacial angles, based on which the crystal's orientations can be assigned in many cases. Note, however, that this procedure strictly necessitates that the sample is aligned perpendicular to the viewing direction while at the same time perspective aberrations of the optical system have to be kept at a minimum.

[18] a) R. Oldenbourg, G. Mei, *J. Microsc.* **1995**, *180*, 140–147; b) R. Oldenbourg, *Nature* **1996**, *381*, 811–812.

[19] M. Born, E. Wolf, *Principles of Optics, 6th ed.*, Pergamon, Oxford, **1986**, p. 699. Compared to Equation (36) given in the textbook, the formula presented here omits the factor $(2\pi/\lambda)$ to obtain δ directly in nm, after entering ρ in nm.

[20] G. Gosh, *Opt. Commun.* **1999**, *163*, 95–102.

[21] Since the optical axis of calcite coincides with its crystallographic *c* axis, the angle parameter ϑ is obtained from calculating angles between pairs of (00.1) and (*hk.l*) crystal planes represented by Miller indexes. Calculations were conveniently performed with two public domain software tools located at http://www.public.asu.edu/~bdegreg/Xtalplanes.html, and http://www.jcrystal.com/steffenweber/JAVA/juvw/JCELL.html. (Calcite unit cell parameters: $a=b=4.988$, $c=17.068$ Å, $\alpha=\beta=90°$, $\gamma=120°$). Full analytical expressions are given in the *International Tables for X-Ray Crystallography, Vol. II*, IUCr, Kynoch, Birmingham, **1972**, p. 168. Computed ϑ values are as follows: 63.2° {01.2}, 44.7° {10.4}, 90.0° {11.0}, 66.3° {11.3}, 75.8° {20.2}, 48.8° {11.6}, 21.6 {10.10}, 26.3° {11.8}.

[22] a) A. Sellinger, P. M. Weiss, A. Nguyen, Y. F. Lu, R. A. Assink, W. L. Gong, J. C. Brinker, *Nature* **1998**, *394*, 256–260; b) Z. Tang, N. A. Kotov, S. Magonov, B. Ozturk, *Nat. Mater.* **2003**, *2*, 413–418.

[23] a) G. Xu, N. Yao, I. A. Aksay, J. T. Groves, *J. Am. Chem. Soc.* **1998**, *120*, 11977–11985; b) E. DiMasi, V. M. Patel, M. Sivakumar, M. J. Olszta, Y. P. Yang, L. B. Gower, *Langmuir* **2002**, *18*, 8902–8909.

[24] N. Hosoda, T. Kato, *Chem. Mater.* **2001**, *13*, 688–693.

[25] A. Sugawara, T. Kato, *Chem. Commun.* **2000**, 487–488.

[26] S. Mann, G. A. Ozin, *Nature* **1996**, *382*, 313–318.

[27] J. Aizenberg, D. A. Muller, J. L. Grazul, D. R. Hamann, *Science* **2003**, *299*, 1205–1208.

[28] A. A. Zakhidov, R. H. Baughman, Z. Iqbal, C. X. Cui, I. Khayrullin, S. O. Dantas, I. Marti, V. G. Ralchenko, *Science* **1998**, *282*, 897–901.

[29] a) A. R. Parker, R. C. McPhedran, D. R. McKenzie, L. C. Botten, N. A. P. Nicorovici, *Nature* **2001**, *409*, 36; b) S. Kinoshita, S. Yoshioka, K. Kawagoe, *Proc. R. Soc. London Ser. B* **2002**, *269*, 1417–1421.

[30] R. Giles, S. Manne, S. Mann, D. E. Morse, G. D. Stucky, P. K. Hansma, *Biol. Bull.* **1995**, *188*, 1–15.

[31] L. Addadi, S. Raz, S. Weiner, *Adv. Mater.* **2003**, *15*, 959–970.